

Identification of a Novel Splice Site Mutation of the *CSPG2* Gene in a Japanese Family with Wagner Syndrome

Tatsuro Miyamoto,^{1,2} Hiroshi Inoue,¹ Yukiko Sakamoto,¹ Eiji Kudo,¹ Takeshi Naito,² Takako Mikawa,³ Yoichi Mikawa,³ Yasushi Isashiki,⁴ Dai Osabe,⁵ Shuichi Shinohara,⁵ Hiroshi Shiota,² and Mitsuo Itakura¹

PURPOSE. To investigate the genetic basis and clinical variability of Wagner syndrome, a rare, dominantly inherited vitreoretinopathy.

METHODS. Clinical examination, linkage analysis, and mutational screening were performed in a large, three-generation, consanguineous Japanese family with Wagner syndrome. The effect of splice site mutation was assessed by reverse transcriptase-polymerase chain reaction (RT-PCR) analysis with lymphoblastoid cell total RNAs generated from affected individuals.

RESULTS. Ocular phenotypes of affected members included an empty vitreous with fibrillary condensations, avascular membrane, perivascular sheathing, and progressive chorioretinal dystrophy and were similar to those of the original Wagner syndrome family. All affected eyes examined exhibited pseudoechotopia with ectopic fovea. No systemic manifestations were observed. Genetic linkage confirmed disease segregation with the previously identified *WGN1* locus on 5q13-q14. A heterozygous A→G transversion at the second base of the 3'-acceptor splice site of intron 7 (c.4004-2 A→G) of the chondroitin sulfate proteoglycan 2 (*CSPG2*) gene that cosegregated with the disease was identified. Results of RT-PCR analysis indicated that the c.4004-2 A→G mutation activates a cryptic splice site, located 39 bp downstream from the authentic 3' splice acceptor site.

CONCLUSIONS. This linkage study confirmed the genetic homogeneity of the Wagner syndrome. *CSPG2* encodes versican, a large chondroitin sulfate proteoglycan, which, in vitreous, binds to hyaluronan and link protein and forms large aggregates that are important for maintaining structural integrity. Although the *CSPG2* gene has been excluded as a candidate for causing Wagner syndrome, these data emphasize the necessity

of further mutational screening in new families and careful functional characterization. (*Invest Ophthalmol Vis Sci.* 2005; 46:2726-2735) DOI:10.1167/iov.05-0057

Wagner syndrome (OMIM 143200; Online Mendelian Inheritance in Man; <http://www.ncbi.nlm.nih.gov/Omim/> provided in the public domain by the National Center for Biotechnology Information, Bethesda, MD), a dominantly inherited vitreoretinopathy, was first reported in 1938 as "hereditary hyaloid retinal degeneration."¹ In most patients with this syndrome, an optically empty vitreous cavity, secondary to vitreous degeneration, and a preretinal avascular membrane are the initial clinical presentations. Both usually occur during childhood or adolescence. Other optical features, including progressive chorioretinal atrophy, perivascular sheathing, subcapsular cataract, and myopia,¹⁻³ increase with age and are frequently associated with severe visual impairment.

Several disorders resembling Wagner syndrome have been described. These include Stickler syndrome,⁴ autosomal dominant erosive vitreoretinopathy,⁵ Goldmann-Favre disease,⁶ and Marshall syndrome.⁷ Because many clinical features of these disorders overlap, there has been considerable confusion as to the individual disease entities. Stickler syndrome is an autosomal dominant connective tissue disorder characterized by orofacial, skeletal, and auditory disorders, in addition to ocular manifestations. Mutations causing Stickler syndrome are most commonly found in the type II collagen (*COL2A1*) gene located on chromosome 12.⁸⁻¹⁰ Since the original report by Wagner, many families have been described as having Wagner syndrome with systemic features also found in Stickler syndrome, and the differentiation of these two entities has been controversial. Indeed, some researchers have suggested the two to be the same disorder and the term "Wagner-Stickler syndrome" has been proposed. However, a recent finding of genetic linkage to 5q13-q14 (the *WGN1* locus) in the original Wagner syndrome family and exclusion of linkage to the *COL2A1* gene confirmed that Wagner syndrome, showing only ocular manifestations, is a condition distinct from Stickler syndrome.¹¹⁻¹⁴ Further clinical studies have indicated that, in addition to the difference in systemic manifestations absent from Wagner syndrome, the frequencies of retinal detachment (RD) and retinal degeneration, as well as the extent of myopia, differ between the two syndromes.^{3,15} In a further confusing finding, an atypical form of Stickler syndrome with minimal or no extraocular manifestations was reported with *COL2A1* exon 2 mutations. Lack of significant systemic manifestations was consistent with selective tissue expression of the major *COL2A1* isoform in nonocular tissues, with exon 2 spliced out of this gene.¹⁵⁻¹⁷ Autosomal dominant erosive vitreoretinopathy also shows some similarities to Wagner syndrome. It has a higher incidence of rhegmatogenous RDs than does Wagner syndrome, but lacks systemic features such as those in Stickler syndrome.⁵ Both Wagner syndrome and erosive vitreoretinopathy have been mapped to 5q13-q14, indicating that erosive

From the ¹Division of Genetic Information, Institute for Genome Research, and the ²Department of Ophthalmology and Visual Neuroscience, Institute of Health Biosciences, The University of Tokushima, Tokushima, Japan; the ³Mikawa Eye Clinic, Tokushima, Japan; the ⁴Department of Ophthalmology, Kagoshima University Faculty of Medicine, Kagoshima, Japan; and the ⁵Department of Bioinformatics, Division of Life Science Systems, Fujitsu, Ltd., Tokyo, Japan.

Submitted for publication January 17, 2005; revised February 22, 2005; accepted March 22, 2005.

Disclosure: **T. Miyamoto**, None; **H. Inoue**, None; **Y. Sakamoto**, None; **E. Kudo**, None; **T. Naito**, None; **T. Mikawa**, None; **Y. Mikawa**, None; **Y. Isashiki**, None; **D. Osabe**, Fujitsu, Ltd. (E); **S. Shinohara**, Fujitsu, Ltd. (E); **H. Shiota**, None; **M. Itakura**, None

The publication costs of this article were defrayed in part by page charge payment. This article must therefore be marked "advertisement" in accordance with 18 U.S.C. §1734 solely to indicate this fact.

Corresponding author: Hiroshi Shiota, Department of Ophthalmology and Visual Neuroscience, Institute of Health Biosciences, The University of Tokushima Graduate School, 3-18-15 Kuramoto-cho, Tokushima 770-8503, Japan; shiota@clin.med.tokushima-u.ac.jp.

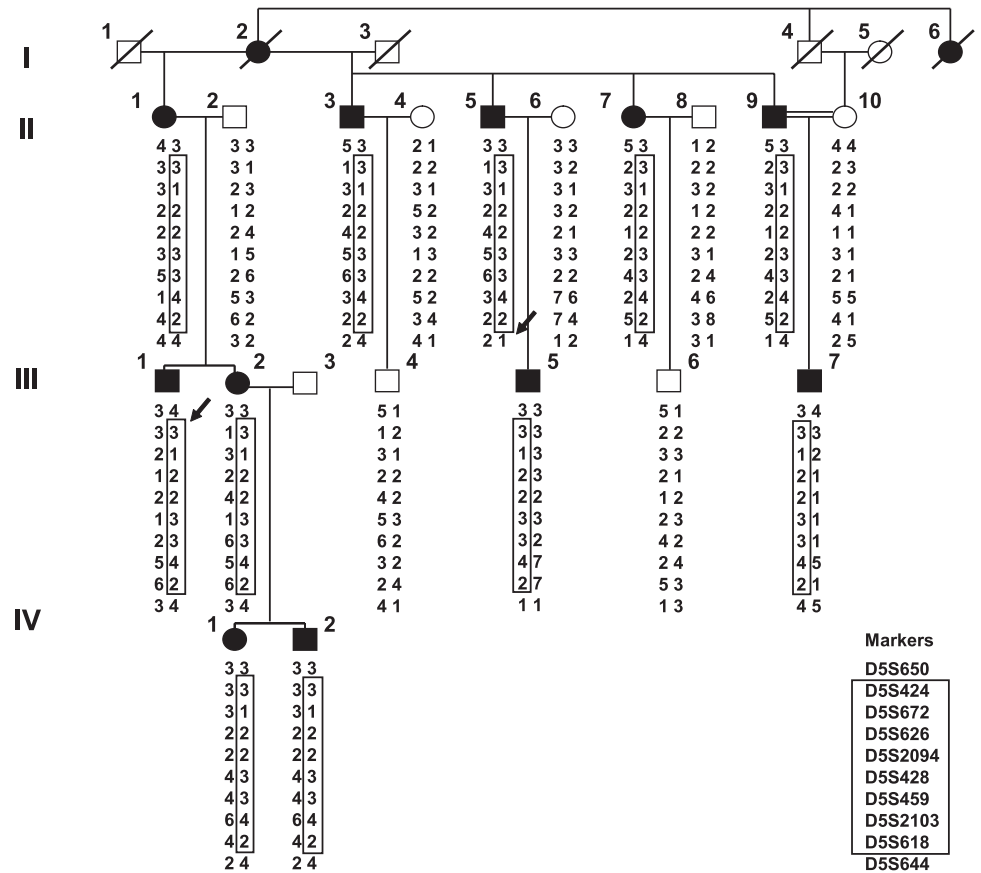


FIGURE 1. A large, three-generation, consanguineous Japanese family with Wagner syndrome (Tokushima pedigree). *Solid symbols:* affected individuals. Genotypes for 10 chromosome 5 markers are shown below the individuals. Alleles forming the reconstructed disease-associated haplotype (3-1-2-2-3-3-4-2) are grouped and *boxed* to demonstrate co-inheritance with the disease phenotype. *Arrows:* key recombination events in II-5 and III-1 are indicated.

vitreoretinopathy may be an allelic variant of Wagner syndrome.¹¹

To date, the disease gene for Wagner syndrome has not been identified. The minimum critical region for Wagner syndrome was reported to be an approximately 2.5-cM genomic interval at 5q14.¹⁴ In this study, using a large and well-characterized Japanese Wagner family, we confirmed linkage to the *WGN1* locus. We found a novel splicing mutation in the *CSPG2*/versican gene, which encodes important extracellular matrix component of the vitreous gel and a promising candidate for the Wagner syndrome gene. The mutation perfectly cosegregated with the disease phenotype and was not present in control individuals. We also demonstrated some evidence supporting functional significance of the mutation.

METHODS

Family and Controls

The study was conducted in accordance with the tenets of the Declaration of Helsinki. With the approval of the Ethics Committee for Human Genomic DNA Research, School of Medicine, the University of Tokushima, we collected clinical data and blood samples from 18 members of a large three-generation consanguineous Japanese family with Wagner syndrome (Tokushima pedigree; Fig. 1). There were 11 affected individuals, 2 unaffected individuals, and 5 spouses who served as control subjects. Prior written and informed consent was obtained from all participants. Genomic DNA was extracted from peripheral blood leukocytes by a standard phenol-chloroform method. Immortalized lymphoblastoid cell lines were also established with the infection of Epstein-Barr virus at the Special Reference Laboratories, Inc. (Tokyo, Japan). We examined frequencies of nucleotide changes or mutations, identified during the study, in 250 unrelated Japanese control individuals living in Tokushima Prefecture, Japan.

Genotyping and Linkage Analysis

Linkage analysis of candidate chromosomes 5 and 12 was performed by linkage mapping (Prism Linkage Mapping Set, ver. 2.0; Applied Biosystems, Inc. [ABI], Foster City, CA). The initial average marker spacings were 5 cM (chromosome 5) and 10 cM (chromosome 12). For chromosome 5, additional markers (*D5S2046*, *D5S637*, *D5S650*, *D5S626*, *D5S2094*, *D5S459*, and *D5S2103*) registered in the Marshfield human genetic linkage map were used for high-density mapping (<http://www.marshfieldclinic.org/research/> provided in the public domain by Marshfield Laboratories, Marshfield, WI). Genotyping was performed as described elsewhere.¹⁸ Briefly, fluorescence-labeled polymerase chain reaction (PCR) products were separated by electrophoresis (model 3700 DNA Analyzer; analyzed by Genescan, ver. 3.7, and Genotyper, ver. 2.1 software; ABI). Two-point linkage analysis was performed with the MLINK program, version 5.1, from the LINKAGE computer program (<http://www.hgmp.mrc.ac.uk/>; provided in the public domain by the Human Genome Mapping Project Resources Centre, Cambridge, UK). A consanguinity loop in the Tokushima pedigree was broken at the individual II-10. Lod scores were generated assuming autosomal dominant inheritance with a penetrance of 90% or 100%. The affected allele frequency was taken as 0.0001. Marker allele frequencies were assumed to be equal. Multipoint analyses were performed using the FASTLINK program (<http://softlib.cs.rice.edu/> provided in the public domain by Rice University, Houston, TX). Microsatellite haplotype construction was performed with visual inspection and with the GeneHunter linkage program, version 2.1_r2 beta (<http://linkage.rockefeller.edu/soft/gh/> provided in the public domain by Rockefeller University, New York, NY) using the order reported by the Marshfield chromosome 5 sex-averaged linkage map¹⁹ and the National Center for Biotechnology Information (NCBI) Map Viewer (<http://www.ncbi.nlm.nih.gov/mapview/build34/> provided in the public domain by NCBI, Bethesda, MD).

Mutational Screening by PCR Direct-Sequencing Analysis

Genes located within the Wagner syndrome minimum critical region¹³ on 5p14 were screened for mutations by PCR direct-sequencing analysis. According to the sequence annotation databases (NCBI Map Viewer and UCSC Browser: <http://genome.ucsc.edu/> provided in the public domain by the University of California at Santa Cruz, Santa Cruz, CA), these included eight known genes (*CSPG2*, *HAPLN1*, *EDIL3*, *XRCC4*, *COX7C*, *RASAI*, *CCNH*, and *MEF2C*) and three hypothetical genes (*MGC23909*, *FLJ11292*, and *MGC33214*). PCR primers, to amplify exons and intron-exon boundaries, were designed on computer (Oligo, ver. 6 software; Molecular Biology Insights, Inc., Cascade, CO; Supplementary Table S1, available online at <http://www.iovs.org/cgi/content/full/46/8/2726/DC1>). DNAs from three patients (II-1, II-5, and III-1) and three control subjects (II-2, III-4, and III-6) from the Tokushima pedigree were used for initial mutational screening. PCR was performed (Ampli Taq Gold; ABI, or Platinum Taq ; Invitrogen, Carlsbad, CA), according to the manufacturers' instructions, in a DNA thermal cycler (model 9700; PerkinElmer, Wellesley, MA). After the reaction, PCR products were purified to eliminate the primers and dNTPs (ExoSAP-IT; Amersham Pharmacia, Biotech, Piscataway, NJ) and were directly sequenced by dye termination chemistry (Prism BigDye Terminator and Sequencing kit, ver. 1, and model 3100 Gene Analyzer; ABI). To evaluate the prevalence of the c.4004-2 A→G mutation in the *CSPG2* gene, DNAs from 250 unrelated control individuals were subjected to PCR direct-sequencing analysis with primers CSPG28-1F and CSPG28-1bR (Supplementary Table S2, available online at <http://www.iovs.org/cgi/content/full/46/8/2726/DC1>).

RT-PCR and Real-Time Quantitative RT-PCR Analysis

Total RNA was extracted from cultured lymphoblastoid cells (II-3, II-4, II-5, II-6, II-7, II-8, III-4, III-5, and III-6) with a commercial system (RNeasy; Qiagen, Santa Clara, CA) and then reverse-transcribed using oligo-dT primer and reverse transcriptase (Superscript III; Invitrogen). To evaluate the expression patterns of four known splice variants of the *CSPG2* gene,²⁰ sets of primers were designed based on the variable exon usage of each variant (V0, 71F and 81R; V1, 61F and 81R; V2, 71F and 91R; and V3, 61F and 91R; Supplementary Table S3, available online at <http://www.iovs.org/cgi/content/full/46/8/2726/DC1>). Primers specific for the *GAPDH* gene were used in positive control experiments. RT-PCR amplification processes consisted of an initial denaturation step at 95°C for 10 minutes, followed by 35 cycles of denaturing at 95°C for 1 minute, annealing at 55°C for 1 minute, extension at 72°C for 1 minute, and a final extension step at 72°C for 10 minutes. All products were run on 8% polyacrylamide gels or 3% agarose gels (Metaphor; FMC Corp., Rockland, ME) and stained with ethidium bromide. Aberrant cDNA fragments of V0 and V1 splice variants due to the *CSPG2* c.4004-2 A→G mutation were gel purified (Gel Extraction MinElute Kit; Qiagen), cloned into a vector (PCRII-TOPO; Invitrogen), and sequenced on a gene analyzer (model 3100 Gene Analyzer; ABI).

Quantification of gene expression was performed with the 5' nuclease ($TaqMan$) assay (Prism 7900HT Sequence Detection System; ABI). Pair-wise primers and probes were designed (Primer Express software, ver. 1.0; ABI). To detect each *CSPG2* splice variant separately, $TaqMan$ probes were designed specifically to span exon-exon junctions that were unique for each splice variant (V0 probe, exon 7-8; V1 probe, exon 6-8; V2 probe, exon 7-9; and V3 probe, exon 6-9). The sequences of the PCR primers and probes are provided in Supplementary Table S3 (available online at <http://www.iovs.org/cgi/content/full/46/8/2726/DC1>). Probes were dual labeled at the 5'-end with the reporter dye molecule FAM (6-carboxy-fluorescein) or VIC, and at the 3'-end with the quencher dye molecule TAMRA (6-carboxy-tetramethyl-rhodamine). All primers and probes were synthesized by ABI. A predesigned $TaqMan$ probe and primer set for the human *CSPG2* gene (Assay ID, Hs00171642_m1; ABI), which detect all *CSPG2* splice variants simultaneously, was obtained from ABI. Human total RNAs were

obtained from various commercial sources: Human Total RNA Master Panel II (BD Biosciences, San Jose, CA), retinal cDNA (QUICK-Clone; BD Biosciences) and the Universal Human Reference Total RNA (BD Biosciences). The Universal Human Reference Total RNA was made by pooling the total RNAs from a collection of various tissues, which provided the standardization of gene expression profile. First-strand cDNA was synthesized from 2 μ g of total RNA (Superscript III First-Strand Synthesis System; Invitrogen). Two nanograms of cDNA template was combined with PCR master mix (1 \times $TaqMan$ Universal PCR MasterMix, without AmpErase UNG; ABI), 200 nM forward and reverse primers, and 250 nM probe. PCR reactions were performed in triplicate in an optical 384-well plate (MicroAmp) in a total volume of 20 μ L on a sequence-detection system (Prism 7900HT; ABI). The cycle conditions were: 95°C for 10 minutes, followed by 40 cycles of 95°C for 15 seconds and 60°C for 1 minute. Data were collected with instrument spectral compensations (SDS 2.1 software; ABI) and analyzed using the threshold cycle (Ct) relative quantification method (ABI). Expression levels of each *CSPG2* splice variant mRNA were normalized by reference to the level of β -actin expression (Human β -actin, cat. no. 4310881E; ABI).

Splice-Site Score

The sequence environment of the c.4004-2 A→G mutation at the 3' acceptor splice site of intron 7 of the *CSPG2* gene was analyzed by using the NNSPLICE program, ver. 0.9 (http://www.fruitfly.org/seq_tools/splice.html/ provided in the public domain by the Berkeley Drosophila Genome Project, Berkeley, CA),²¹ and the splice-site scores (SSSs) for a normal site (SSS-nor), a mutated site (SSS-mut), and a cryptic site (SSS-crypt) were calculated.

RESULTS

Ocular Phenotypes of Wagner Syndrome Patients

We assessed a three-generation consanguineous Japanese family with Wagner syndrome (Tokushima pedigree, Fig. 1). Clinical findings in the patients are summarized in Table 1. Overall, ocular phenotypes were very similar to those described in the original report by Wagner,¹ and included an empty vitreous with fibrillary condensations in the vitreous cavity, avascular membrane (stands and veils, Fig. 2A), perivascular sheathing or obliteration (Fig. 2B), and progressive chorioretinal dystrophy with pigmentation. None of the orofacial, auditory, and skeletal manifestations, often seen in patients with Stickler syndrome, was observed. RD was observed in three eyes of three patients (III-5, IV-1, and IV-2). In patients IV-1 and IV-2, detached retinas were successfully treated with improvement of vision by vitrectomy or scleral buckling. Patient III-5 had congenital tractional RD with no light perception in his right eye. There were no indications for surgery in this case. All affected eyes examined had ectopic fovea and associated pseudoexotropia, showing a high angle gamma of nearly +10° and a 5 to 10° deviation of Mariotte's blind spot to the temporal side (Fig. 2C). Para-central and ring scotomas were observed in all affected eyes examined (Figs. 2C, 2D). Subnormal electroretinographic (ERG) responses due to progressive chorioretinal changes, typically with a initial reduction of oscillatory potential (OP) followed by reduced a- and b-wave amplitudes, were observed in patients II-5, II-7, II-9, III-1, III-2, and III-7. In patients IV-1 and IV-2, ERGs were nonrecordable in their left eyes because of RD.

Confirmation of Wagner Syndrome Linkage to 5q13-q14

We performed linkage analyses on the Tokushima Wagner pedigree (Fig. 1) focusing on chromosomes 5 and 12, which contain two candidate loci for Wagner syndrome and Stickler

TABLE 1. Clinical Information on 11 Affected Individuals of Tokushima Pedigree

Patient	Sex	Age at Diagnosis (y)	Visual Acuity	Spherical Equivalent (D)	Operation	Cataract	Empty Vitreous	Avascular Membrane	Chorioretinal Atrophy	Retinal Detachment	Ectopic Fovea			ERG
											Angle Gamma	Dev. of Blind Spot	Visual Field	
II-1	F	35	R 0.70	+15.5	ICCE	Aphakia	+	+	+	-	+11°	5°	RS	Sub
			L 0.80	+16.5	ICCE	Aphakia	+	+	+	-	+10°	5°	RS	Sub
II-3	M	29	R 0.60	-4.00	-	+	+	+	+	-	+9°	5°	N/A	Sub
			L 0.60	-1.00	-	+	+	+	+	-	+8°	7°	N/A	Sub
II-5	M	28	R 0.60	+10.0	ICCE	Aphakia	+	+	+	-	+9°	5°	RS	Sub
			L 1.20	+10.5	ICCE	Aphakia	+	+	+	-	+8°	5°	RS	Sub
II-7	F	34	R 1.20	+10.0	ICCE	Aphakia	+	+	+	-	N/A	N/A	RS	Sub
			L 0.90	+7.25	ECCE	Aphakia	+	+	+	-	N/A	N/A	RS	Sub
II-9	M	30	R LP	N/A	-	+	N/A	N/A	N/A	-	N/A	N/A	RS	Sub
			L LP	N/A	-	+	N/A	N/A	N/A	-	N/A	N/A	N/A	Sub
III-1	M	15	R 1.00	+0.50	PEA + IOL	Pseudo	+	+	+	-	+10°	7°	RS	Sub
			L 0.02	-1.50	PEA + IOL	Pseudo	+	+	+	-	+12°	7°	RS	Sub
III-2	F	14	R 1.00	-9.00	-	+	+	+	+	-	+4°	5°	PS	Sub
			L 0.90	-1.00	PEA + IOL	Pseudo	+	+	+	-	+4°	5°	PS	Sub
III-5	M	2	R NLP	N/A	-	+	+	+	+	TRD	n.d.	N/A	N/A	N/A
			L 0.90	-0.5	-	+	+	+	+	-	n.d.	N/A	N/A	N/A
III-7	M	2	R 0.10	+8.00	ICCE	Aphakia	+	+	+	-	+12°	N/A	RS	Sub
			L 0.70	-4.00	PEA + IOL	Pseudo	+	+	+	-	+10°	N/A	RS	Sub
IV-1	F	11	R 0.60	-4.50	-	+	+	+	+	-	N/A	N/A	N/A	Sub
			L 0.40	+11.5	vitrectomy	Aphakia	+	+	+	RRD	N/A	N/A	N/A	NR
IV-2	M	11	R 0.80	-0.50	-	+	+	+	+	-	N/A	5°	PS	Sub
			L 0.10	-4.00	sc.buckling	+	+	+	+	RRD	N/A	N/A	RS	NR

There were no systemic diseases in the patients. ERG, electroretinogram; LP, light perception; NLP, no light perception; ICCE, intracapsular cataract extraction; ECCE, extracapsular cataract extraction; PEA, phaco-emulsification and aspiration; IOL, intraocular lens implantation; sc.buckling, scleral buckling; Pseudo, pseudo-phakia; TRD, tractional retinal detachment; RRD, rhegmatogenous retinal detachment; RS, ring scotoma; PS, paracentral scotoma; Sub, subnormal ERG; NR, non-recordable ERG; N/A, not assessed.

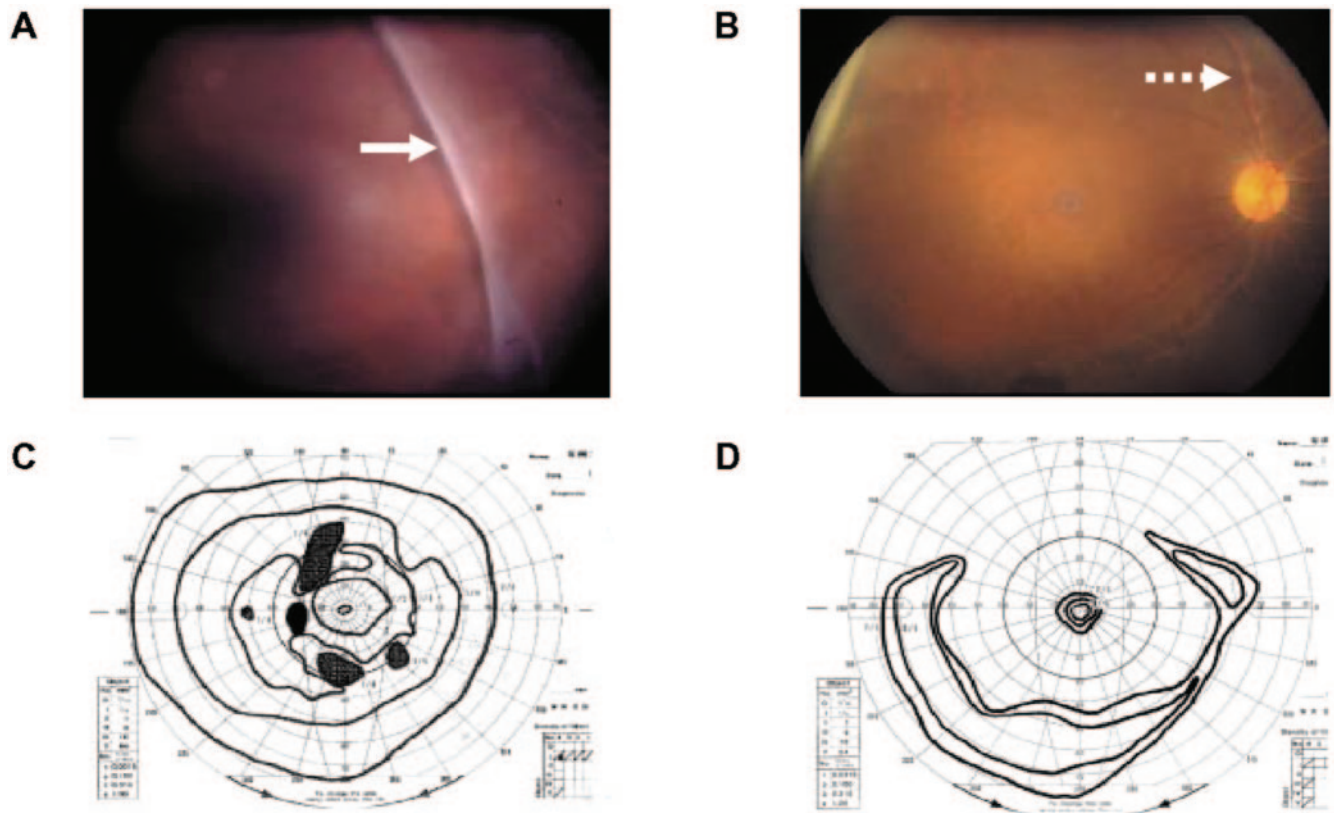


FIGURE 2. Fundus photographs and results of Goldmann perimeter test. The right eye (III-2), with avascular membrane (A, arrow) and chorioretinal dystrophy and perivasculopathy (B, dashed arrow), is shown. A 5° deviation of Mariotte's blind spot to the temporal side and paracentral scotomas was present in the left eye (C, III-2). Progressive chorioretinal atrophy has resulted in the formation of a ring scotoma (D, II-5).

syndrome (5q13-q14; *WGN1* locus and 12q12; *COL2A1* gene, respectively). Eighteen family members including 11 affected individuals, 2 unaffected individuals, and 5 spouse control subjects were genotyped. Significant evidence of linkage (i.e., $Z > 3.0$ at $\theta = 0.0$) was obtained with markers on 5q13-q14, whereas the *COL2A1* locus was entirely excluded from linkage. The maximum two-point lod scores were obtained with markers *D5S459* ($Z = 3.01$, $\theta = 0$) and *D5S2103* ($Z = 3.06$, $\theta = 0$) and are summarized in Table 2. Multipoint linkage analysis resulted in the maximum lod score of 3.48 between markers *D5S459* and *D5S2103* (Fig. 3). Haplotype construction and analyses indicate a disease-associated haplotype (3-1-2-2-3-3-4-2) with eight short tandem repeat (STR) markers

(*D5S424*, *D5S672*, *D5S626*, *D5S2094*, *D5S428*, *D5S459*, *D5S2103*, *D5S618*; Fig. 1). Informative chromosomal recombinants observed in patients II-5 and III-1 narrowed the minimum genetic region to a 26.5-cM interval between *D5S650* and *D5S644*. The region completely encompassed the reported critical region for *WGN1* within the 2- to 2.5-cM interval between markers *D5S626* and *HAPLN1* (*CRTL1AC*).^{13,14}

Identification of a Splicing Mutation in the *CSPG2* Gene

Our present genetic studies confirmed the linkage of Wagner syndrome to region 5q13-q14 (*WGN1* locus), but failed to

TABLE 2. Two-Point Lod Scores for 5q13-q14 Markers (*WGN1* Locus) and 12q13 Markers (*COL2A1* Locus)

Locus	Microsatellite Marker (Location)	Recombination Fraction (θ)						
		0.00	0.01	0.05	0.1	0.2	0.3	0.4
5q13-q14	<i>D5S650</i> (78.3 cM)	$-\infty$	-0.22	0.34	0.47	0.42	0.26	0.10
	<i>D5S424</i> (82 cM)	2.19	2.15	1.98	1.77	1.35	0.91	0.47
	<i>D5S672</i> (86.3 cM)	1.48	1.44	1.29	1.10	0.73	0.38	0.11
	<i>D5S626</i> (92.4 cM)	0.60	0.58	0.51	0.43	0.27	0.13	0.03
	<i>D5S2094</i> (93.6 cM)	2.29	2.25	2.08	1.86	1.40	0.94	0.48
	<i>D5S428</i> (95.4 cM)	2.37	2.32	2.15	1.92	1.45	0.97	0.48
	<i>D5S459</i> (97.2 cM)	3.01	2.96	2.74	2.46	1.88	1.27	0.64
	<i>D5S2103</i> (97.8 cM)	3.06	3.01	2.79	2.51	1.91	1.29	0.65
	<i>D5S618</i> (99.4 cM)	2.30	2.25	2.07	1.83	1.34	0.85	0.39
	<i>D5S644</i> (104.8 cM)	$-\infty$	-1.61	-0.35	0.09	0.34	0.32	0.19
12q13	<i>D12S85</i> (61.3 cM)	$-\infty$	-4.71	-2.31	-1.26	-0.37	-0.01	0.09
	<i>D12S368</i> (66.0 cM)	$-\infty$	-3.82	-1.85	-1.09	-0.46	-0.18	-0.04

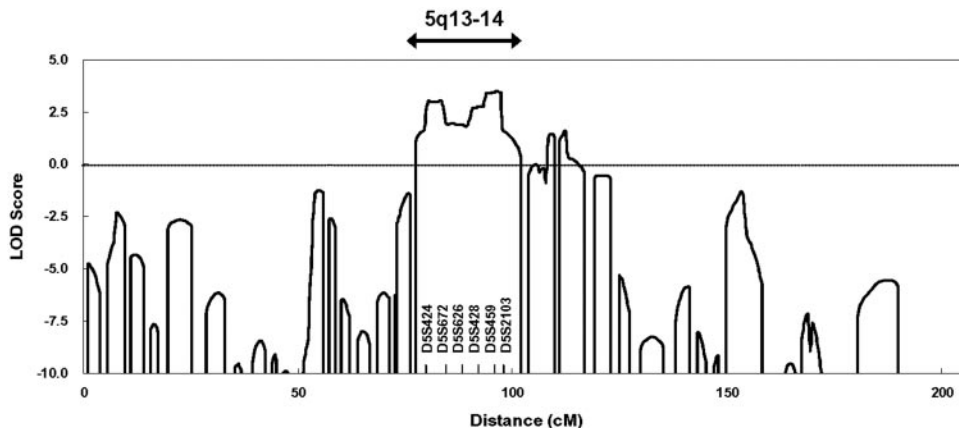


FIGURE 3. Multipoint linkage analysis of chromosome 5 markers of the Tokushima pedigree (fine mapping). *WGN1* locus on 5q13-q14 is shown with markers. Multipoint analyses yielded a maximum lod score of 3.48 between markers *D5S459* and *D5S2103*.

obtain a more narrow localization of the disease gene compared with prior studies.¹⁴ Thus, to identify the causative gene in the Tokushima pedigree, we conducted mutational screening for genes within a 7-cM critical interval flanked by *D5S626* and *D5S2103*, identified by Black et al.¹³ According to the public database, the region contained eight known genes and three hypothetical genes (Fig. 4; see the Methods section). All exons and promoter region were analyzed by PCR direct genomic sequencing. Although several single nucleotide polymorphisms (SNPs) were detected, no pathogenic mutations were identified in *HAPLN1*, *EDIL3*, *XRCC4*, *COX7C*, *RASA1*, *CCNH*, *MEF2C*, *MGC23909*, *FLJ11292*, and *MGC33214* genes (Supplementary Table S4, available online at <http://www.iovs.org/cgi/content/full/46/8/2726/DC1>). The *CSPG2* gene was composed of 15 exons. Sequencing of the *CSPG2* gene revealed a heterozygous A→G transversion at the second base of the 3' acceptor splice site of intron 7 (c.4004-2 A→G) in affected patients (Fig. 5A). The c.4004-2 A→G mutation cosegregated perfectly with the disease phenotype in the Tokushima pedigree and was not present in 250 Japanese normal control subjects (500 chromosomes, data not shown).

Aberrant *CSPG2* Splicing Transcripts

CSPG2 encodes versican, a large proteoglycan aggregating with chondroitin sulfate (CS). Versican binds the CS proteoglycan through two glycosaminoglycan (GAG)-attachment domains, αGAG and βGAG, encoded by exons 7 and 8, respec-

tively.²⁰ Four major *CSPG2*/versican splice variants (V0, V1, V2, and V3) are known (Fig. 4D), and they differ dramatically in the extent of modification by glycosaminoglycan chains. The V0 variant has both αGAG and βGAG domain, whereas V1 and V2 have a single GAG domain (αGAG and βGAG, respectively). The V3 variant has no GAG domain.^{22,23} We speculated that the c.4004-2 A→G of the *CSPG2*/versican gene is responsible for either the use of cryptic splice sites or exon skipping. Because no ocular tissues of our patients were available, we tested this hypothesis by RT-PCR, using total RNAs from immortalized lymphoblastoid cells obtained from affected and control individuals. Variant-specific PCR primers were designed based on variable exon usage of each variant and to amplify as relatively short fragments. With our PCR primers and conditions, we could specifically amplify each variant without amplifying another variant with much larger sizes. We found lymphoblastoid cells in normal individuals to express V0, V1, and V3 variants of *CSPG2*/versican (Fig. 6). With primer sets for V0 and V1, amplification of total RNA from affected individuals yielded two fragments of different sizes (Fig. 6A). Sequence analysis of smaller fragments (mutated alleles) showed exon 8 to lack the first 39 nucleotides (Fig. 6B). Furthermore, comparison of cDNA and genomic sequences indicated a cryptic 3' acceptor splice site (*ag*), located 39 bp downstream from the authentic 3' splice acceptor site, to be activated in the presence of the c.4004-2 A→G mutation. The SSS-crypt, calculated by using the NNSPLICE program, was

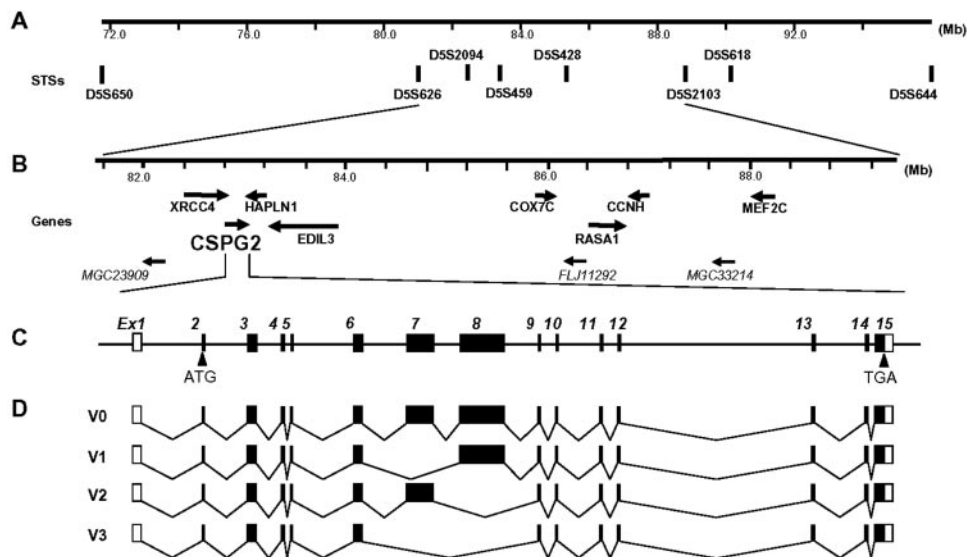


FIGURE 4. Physical and transcript map of Wagner syndrome gene region and genomic structure showing alternative splicing of *CSPG2*. (A) An ~25-Mb region, delimited by the centromeric marker *D5S650* and telomeric marker *D5S644*. The STS marker positions and genes are from the UCSC Browser. (B) Known (*bold text*) and hypothetical (*italic text*) genes, located within the interval between *D5S626* and *D5S2103*, are shown with *arrows* in the direction of transcription. (C) The *CSPG2* gene covers 130 kb of the genomic sequence and consists of 15 exons. (D) Four *CSPG2* gene variants (V0, V1, V2, and V3) differ in the usage pattern of exons 7 and 8, which encode the CSα and CSβ domains, respectively.

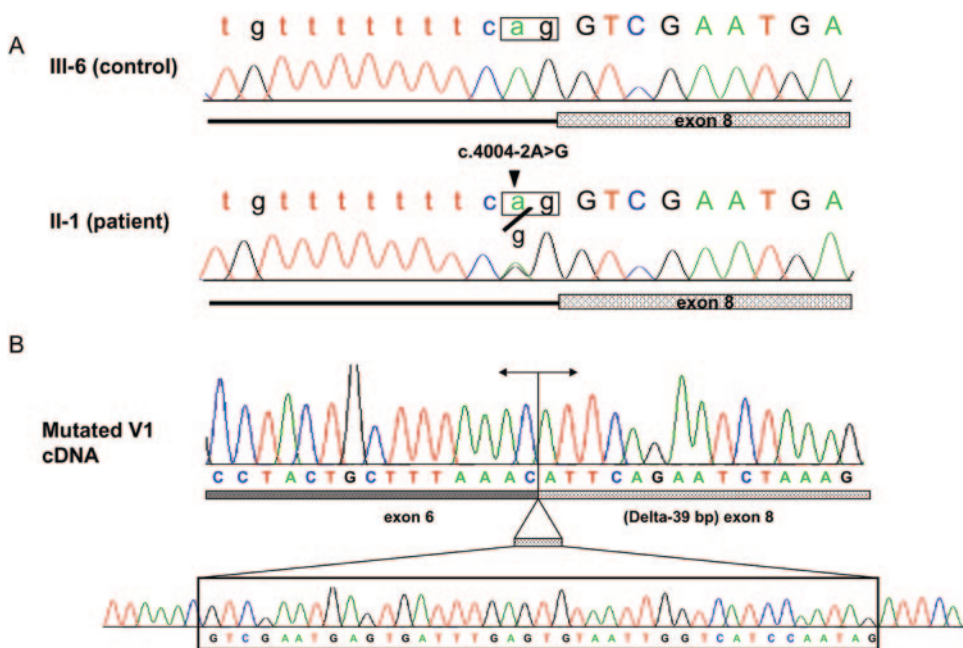


FIGURE 5. (A) Genomic sequencing analysis of the *CSPG2* gene. *Top*: a normal-type sequence around the intron 7–exon 8 boundary of the *CSPG2* gene (III-6; spouse control). *Bottom*: a heterozygous A→G transversion at the second base of the 3′ acceptor splice site of intron 7 (c.4004-2 A→G, II-1; patient). *Box*: the consensus splice acceptor sequence (ag). (B) Aberrant cDNA sequence (V1 variant) caused by the c.4004-2 A→G mutation. RT-PCR products containing the junction of exon 6/exon 8 (V1) were amplified from the patient’s total RNA, subcloned into a vector (PCRII-TOPO; Invitrogen), and sequenced. The mutated V1 transcript lacking the first 39 bp of exon 8 (*bottom*) is shown.

0.05, whereas scores for the authentic acceptor site were 0.99 (SSS-Nor) and 0.00 (SSS-Mut; Fig. 6B). Of note, *de novo* expression of the V2 variant was detected in lymphoblastoid cells only from affected individuals (Fig. 6A).

mRNA Expression of the *CSPG2*/Versican Variants in Retinal Tissue

As a first step in defining the expression pattern of *CSPG2*/versican in human eye structures, we determined the overall distribution pattern of the four *CSPG2*/versican variants in a panel of human tissues by real-time quantitative RT-PCR. As shown in Figure 7, with the *TaqMan* probe Hs00171642_m1 (ABD), designed at the junction between exon 3 and 4 and common to all four variants, a ubiquitous transcription of the *CSPG2*/versican gene was asserted. Expression patterns of each variant were more varied among tissues (Fig. 7): V1 and V3 variants were found to be relatively widespread, whereas the V0 and V2 were less frequently and tissue-specifically

transcribed. Fetal brain predominantly expressed V0, V1, and V2 variants, whereas (adult) whole brain expressed only V2. Heart organ represented the one showing the highest expression levels of *CSPG2*/versican and expressed all variants except for V2. Retinal tissue expressed detectable levels of all *CSPG2*/versican variants, with relatively high expression of the V0 and V3 variants.

DISCUSSION

In this report, we studied the first documented family (Tokushima pedigree) with Wagner syndrome in the Japanese population. The diagnosis was strengthened by detailed clinical information showing the absence of systemic abnormalities in our patients, along with significant evidence of linkage to the previously reported *WGN1* locus (5q13-q14) and exclusion of linkage to the *COL2A1* gene locus (12q13.11-q13.2). It is noteworthy that, in our family, all affected cases exhibited

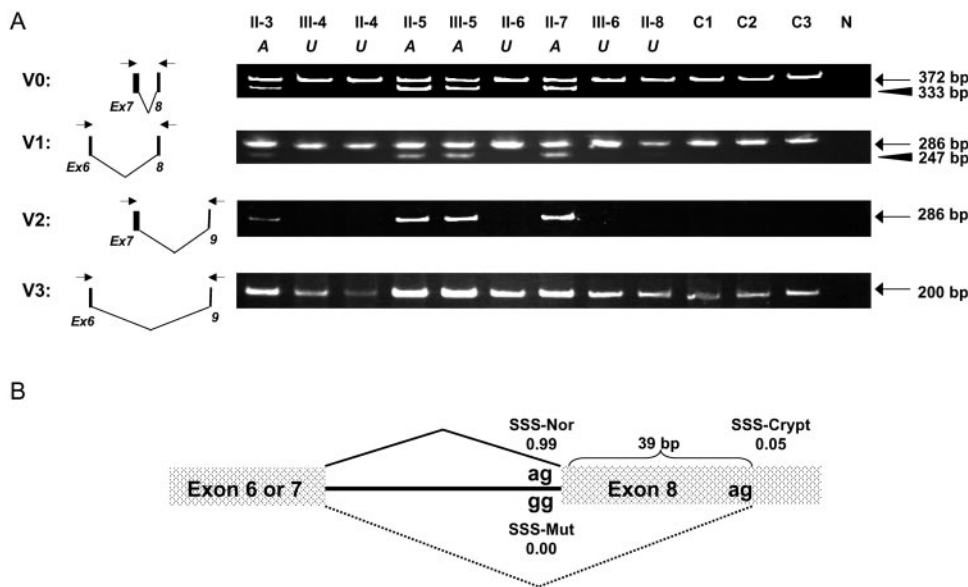


FIGURE 6. (A) RT-PCR analysis on total RNA from cultured lymphoblasts. Each *CSPG2* variant was amplified with variant-specific primer sets (V0, primers 71F and 81R; V1, 61F and 81R; V2, 71F and 91R; and V3, 61F and 91R). Schematic locations of PCR primers are shown on the *right*. Note the extra V0 and V1 fragments (*arrowhead*) with smaller sizes in RNAs from affected individuals (A: II-3, II-5, III-5, and II-7), whereas there are only normal bands (*arrow*) in RNAs from unaffected spouse control subjects (U: III-4, II-4, II-6, III-6, and II-8) and unrelated controls (C1-3). N, no template control. (B) Scheme of aberrant *CSPG2* mRNA splicing. The c.4004-2 A→G mutation activates a cryptic 3′ acceptor splice site (ag), located 39 bp downstream within exon 8 from the authentic 3′ splice acceptor site. SSSs at SSS-Nor, SSS-Mut, and SSS-Crypt are shown.

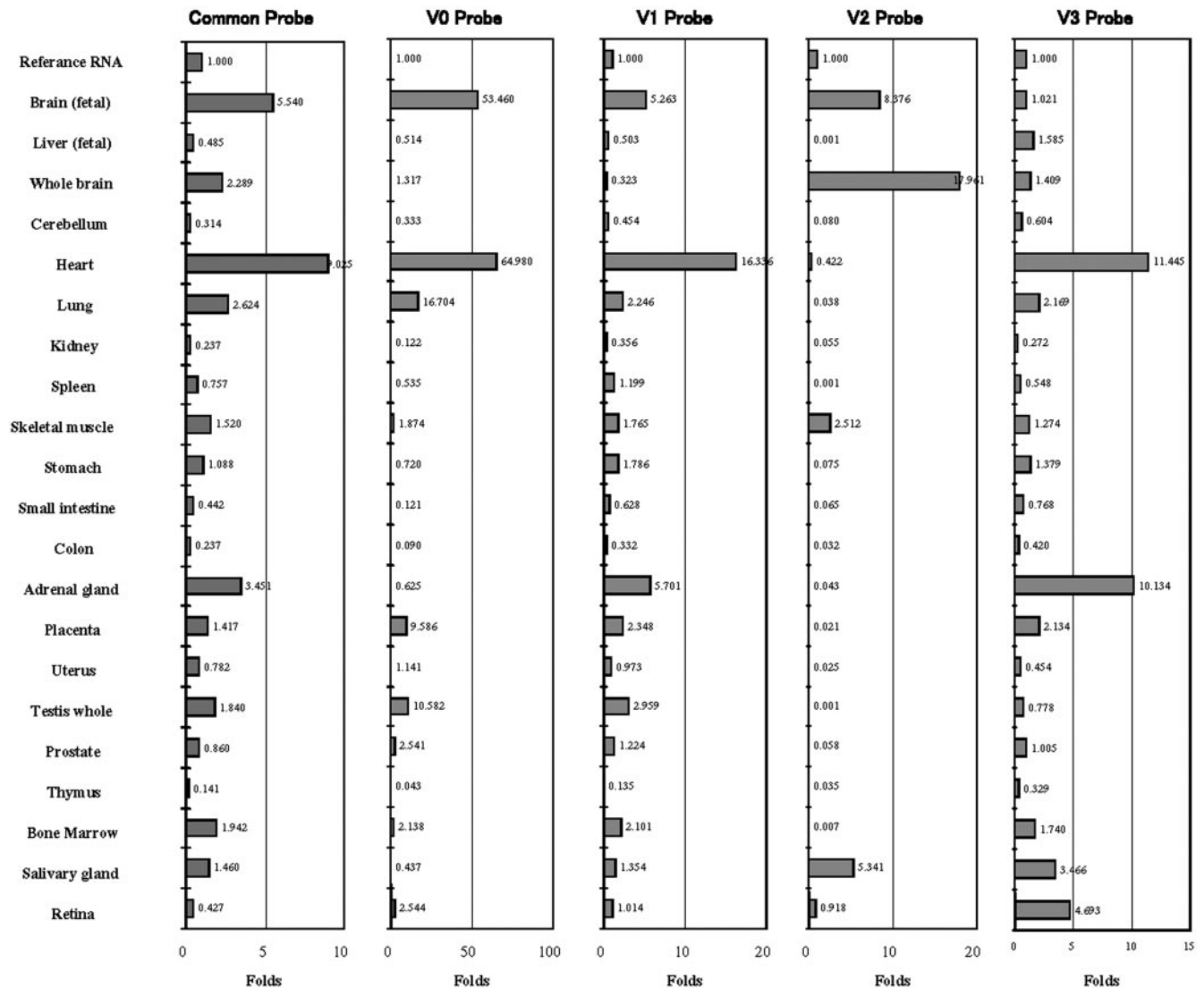


FIGURE 7. Quantitative analysis of *CSPG2*/versican variant expression in normal human tissues. Relative levels of V0, V1, V2, and V3 mRNA expression in the tissues indicated on the *left* are shown. "Common probe" indicates a predesigned probe for the human *CSPG2* gene (TaqMan Assay ID: Hs00171642_m1; ABI), which detect all splice variants simultaneously. Data are presented as the average expression level for each variant mRNA after normalization to expression of β -actin. Expression levels of each variant in the Universal Human Reference Total RNA (BD Biosciences) are set arbitrarily as 1.000.

pseudostrabismus due to ectopic fovea in the temporal direction (Table 1). This heterotopia has not been described in previous reports and may be a previously unrecognized manifestation of this syndrome.

Our genetic results confirmed the genetic homogeneity of the Wagner syndrome on 5q13-q14. By analyses of meiotic recombinants, affected members of the Tokushima pedigree shared a 26.5-cM haplotype with no crossovers to allow more precise mapping. The region completely encompassed the 7-cM interval, a minimum critical region for *WGN1* locus. We were thus tempted to conduct mutational screening for all 11 genes located within the region. We identified a novel splice acceptor site mutation (c.4004-2 A→G), located -2 bases from the normal splice acceptor site in intron 7 of the *CSPG2* gene. The c.4004-2 A→G mutation cosegregated perfectly with the disease phenotype in the Tokushima family and was not present in 500 ethnically matched control chromosomes, suggesting that this sequence variation is not a rare polymorphism. The c.4004-2 A→G mutation abolished the highly conserved consensus AG sequence motif at the splice acceptor site and

may result in exon skipping, activation of cryptic splice sites, creation of a pseudoexon within an intron, or intron retention. Results of our RT-PCR experiments suggested that the mutation activated an aberrant cryptic splice site at 39 bp downstream from the authentic splice acceptor site (Figs. 5, 6). This would result in an in-frame 13 conserved amino acids deletion in the V0 and V1 splice variants (for V1, an additional histidine was created). Exon skipping, however, seemed to be undeniable, since an aberrant upregulation of the V2 splice variant, which could be due to skipping of exon 8, was observed in lymphoblastoid cells only from affected individuals. Supporting this notion, the computer calculated splice site score for cryptic site (SSS-crypt) was considerably low (0.05), which presumably is insufficient for efficient splicing.

It is noteworthy that the c.4004-2 A→G mutation in the *CSPG2* gene is the second mutation found in patients with Wagner syndrome. Perveen et al.¹⁴ reported a study of 18 families consisting of 2 previously published families (W1 and D1) with Wagner syndrome and 16 other families with suggestive linkage. Linkage to chromosome 5q14.3 was indepen-

dently confirmed in four families including W1 and D1, whereas the remaining 14 families were too small to confirm or to exclude linkage. The authors searched for the *CSPG2* gene mutation by the RT-PCR and genomic single-strand conformational polymorphism (SSCP)/heteroduplex analysis of exons. In one 5q14.3-linked family (W2), they identified an A→G missense mutation at position 2331 within exon 7, resulting in an alanine-to-threonine substitution in the αGAG attachment domain. Unfortunately, further details, such as the accession number of the reference sequence and the amino acid number, were not included in their report. In the subsequent report,¹³ family W2 was reported to be a large pedigree of Anglo-Saxon origin, consisting of four affected generations with 13 members with Wagner syndrome. Affected members showed a unique form of vitreoretinopathy associated with a variety of ocular developmental abnormalities, including posterior embryotoxon, congenital glaucoma, iris hypoplasia, congenital cataract, ectopia lentis, microphthalmia, and persistent hyperplastic primary vitreous. The A→G missense mutation at *CSPG2* position 2331 segregated perfectly with the disease phenotype and was not present in 100 normal chromosomes. Given the lack of confirmatory evidence of other mutations in the remaining families, Perveen et al.^{13,14} excluded *CSPG2* from the genes possibly responsible for Wagner syndrome. However, the authors themselves acknowledged in their reports that they could not completely rule out the possibility of clinical and genetic heterogeneity in their 18 families, and, in at least some of their families with linkage to loci except for 5q14.3. It is also possible that certain mutations were overlooked because of their locations in an intronic or regulatory region or due to incomplete sensitivity of the SSCP/heteroduplex analysis.

The *CSPG2* gene encodes versican, a large CS proteoglycan (PG). Functionally, versican consists of a hyaluronan (HA)-binding domain at the amino terminus, two GAG-attachment domains (αGAG and βGAG) in the middle, and a set of epidermal growth factor (EGF)-like, lectinlike, and complement regulatory protein-like (CRP) domains at the carboxyl terminus. Alternative splicing of the *CSPG2* gene generates four major versican splice variants (V0, V1, V2, and V3), which differ markedly in their use of GAG-attachment domains.^{20,22,23} Versican has been identified in the bovine, porcine, and human vitreous.^{24–26} In the vitreous, versican is known to bind to HA and link protein (LP) with high affinity, and forms large aggregates, which along with collagen fibrils are important for maintaining structural integrity. Results of our quantitative real-time RT-PCR experiment indicated that adult retinal tissue expressed detectable levels of all *CSPG2*/versican variants. In the chicken, transient and restricted expression of *CSPG2*/versican mRNA is reported in the neuritis-forming layers of embryonic and developing retinas, with little expression in adult.²⁷ We speculate that the c.4004-2 A→G mutation in the *CSPG2*/versican gene may result in insufficient interactions between versican and various vitreous components, including HA and type II collagen and thereby produce premature syneresis and degeneration in the vitreous gel. To test this hypothesis, functional experiments using mutant and wild-type versican cDNAs are under way in our laboratory.

In summary, we have confirmed linkage to the *WGN1* locus on chromosome 5 in a Japanese family with Wagner syndrome. In affected members, we identified a novel splice acceptor site mutation, c.4004-27 A→G, in the *CSPG2*/versican gene, an excellent candidate for being Wagner syndrome gene. Clearly, until additional independent Wagner syndrome families are identified with mutation(s) in this gene, the assignment should remain tentative. Extensive functional studies on *CSPG2*/versican in vitreous gel construction is also needed to define the exact pathogenic relevance. Those studies will eventually lead

to new insights into the critical in vivo roles of proteoglycan in ocular development in the future.

Acknowledgments

The authors thank the patients with Wagner syndrome and their family members for their cooperation; Naoyuki Kamatani (Tokyo Women's Medical University) for help with the linkage analysis; Kyoko Nomura and Sachiko Yabe (Fujitsu Ltd.) for help with the computational analysis; Maki Moritani and Kiyoshi Kunika (Tokushima University) for technical help; Makoto Kajima and Kayo Shinomiya for providing the DNA samples; and Taiji Sakamoto and Norihito Doi (Kagoshima University) and Masahiro Zako (Aichi Medical University) for helpful discussions.

References

1. Wagner H. Ein bisher unbekanntes Erleiden des Auges, beobachtet im Kanton Zurich. *Klin Monatsbl Augenheilkd.* 1938; 100:840–857.
2. Alexander RL, Shea M. Wagner's disease. *Arch Ophthalmol.* 1965; 74:310–318.
3. Graemiger RA, Niemeyer G, Schneeberger SA, Messmer EP. Wagner vitreoretinal degeneration: follow-up of the original pedigree. *Ophthalmology.* 1995;102:1830–1839.
4. Stickler GB, Belau PG, Farrell FJ, et al. Hereditary progressive arthro-ophthalmopathy. *Mayo Clin Proc.* 1965;40:433–455.
5. Brown DM, Kimura AE, Weingeist TA, Stone EM. Erosive vitreoretinopathy: a new clinical entity. *Ophthalmology.* 1994; 101:694–704.
6. Favre M. Two cases of hyaloid-retinal degeneration. *Ophthalmologica.* 1958;135:604–609.
7. Marshall D. Ectodermal dysplasia: report of kindred with ocular abnormalities and hearing defect. *Am J Ophthalmol.* 1958;45:143–156.
8. Ahmad NN, Ala-Kokko L, Knowlton RG, et al. Stop codon in the procollagen II gene (COL2A1) in a family with the Stickler syndrome (arthro-ophthalmopathy). *Proc Natl Acad Sci USA.* 1991; 88:6624–6627.
9. Ahmad NN, McDonald-McGinn DM, Zackai EH, et al. A second mutation in the type II procollagen gene (COL2A1) causing stickler syndrome (arthro-ophthalmopathy) is also a premature termination codon. *Am J Hum Genet.* 1993;52:39–45.
10. Körkkö J, Ritvaniemi P, Haataja L, et al. Mutation in type II procollagen (COL2A1) that substitutes aspartate for glycine alpha 1-67 and that causes cataracts and retinal detachment: evidence for molecular heterogeneity in the Wagner syndrome and the Stickler syndrome (arthro-ophthalmopathy). *Am J Hum Genet.* 1993;53:55–61.
11. Brown DM, Graemiger RA, Hergersberg M, et al. Genetic linkage of Wagner disease and erosive vitreoretinopathy to chromosome 5q13–14. *Arch Ophthalmol.* 1995;113:671–675.
12. Zech JC, Morlé L, Vincent P, et al. Wagner vitreoretinal degeneration with genetic linkage refinement on chromosome 5q13–q14. *Graefes Arch Clin Exp Ophthalmol.* 1999;237:387–393.
13. Black GC, Perveen R, Wiszniewski W, Dodd CL, Donnai D, McLeod D. A novel hereditary developmental vitreoretinopathy with multiple ocular abnormalities localizing to a 5-cM region of chromosome 5q13–q14. *Ophthalmology.* 1999;106:2074–2081.
14. Perveen R, Hart-Holden N, Dixon MJ, et al. Refined genetic and physical localization of the Wagner disease (WGN1) locus and the genes *CRTL1* and *CSPG2* to a 2- to 2.5-cM region of chromosome 5q14.3. *Genomics.* 1999;57:219–226.
15. Richards AJ, Martin S, Yates JR, et al. COL2A1 exon 2 mutations: relevance to the Stickler and Wagner syndromes. *Br J Ophthalmol.* 2000;84:364–371.
16. Donoso LA, Edwards AO, Frost AT, et al. Identification of a stop codon mutation in exon 2 of the collagen 2A1 gene in a large stickler syndrome family. *Am J Ophthalmol.* 2002;134:720–727.

17. Parma ES, Körkkö J, Hagler WS, Ala-Kokko L. Radial perivascular retinal degeneration: a key to the clinical diagnosis of an ocular variant of Stickler syndrome with minimal or no systemic manifestations. *Am J Ophthalmol.* 2002;134:728-734.
18. Kudo E, Kamatani N, Tezuka O, et al. Familial juvenile hyperuricemic nephropathy: detection of mutations in the uromodulin gene in five Japanese families. *Kidney Int.* 2004;65:1589-1597.
19. Broman KW, Murray JC, Sheffield VC, White RL, Weber JL. Comprehensive human genetic maps: individual and sex-specific variation in recombination. *Am J Hum Genet.* 1998;63:861-869.
20. Wight TN. Versican: a versatile extracellular matrix proteoglycan in cell biology. *Curr Opin Cell Biol.* 2002;14:617-623.
21. Reese MG, Eeckman FH, Kulp D, Haussler D. Improved splice site detection in genie. *J Comp Biol.* 1997;4:311-323.
22. Dours-Zimmermann MT, Zimmermann DR. A novel glycosaminoglycan attachment domain identified in two alternative splice variants of human versican. *J Biol Chem.* 1994;269:32992-32998.
23. Zako M, Shinomura T, Ujita M, Ito K, Kimata K. Expression of PG-M (V3), an alternatively spliced form of PG-M without a chondroitin sulfate attachment in region in mouse and human tissues. *J Biol Chem.* 1995;270:3914-3918.
24. Reardon A, Heinegård D, McLeod D, Sheehan JK, Bishop PN. The large chondroitin sulphate proteoglycan versican in mammalian vitreous. *Matrix Biol.* 1998;17:325-333.
25. Noulas AV, Theocharis AD, Feretis E, Papageorgakopoulou N, Karamanos NK, Theocharis DA. Pig vitreous gel: macromolecular composition with particular reference to hyaluronan-binding proteoglycans. *Biochimie (Paris).* 2002;84:295-302.
26. Theocharis AD, Papageorgakopoulou N, Feretis E, Theocharis DA. Occurrence and structural characterization of versican-like proteoglycan in human vitreous. *Biochimie (Paris).* 2002;84:1237-1243.
27. Zako M, Shinomura T, Miyaishi O, Iwaki M, Kimata K. Transient expression of PG-M/versican, a large chondroitin sulfate proteoglycan in developing chicken retina. *J Neurochem.* 1997;69:2155-2161.